

Absolute rate constant determinations for the deactivation of $O(^1D)$ by time resolved decay of $O(^1D) \rightarrow O(^3P)$ emission

J. A. Davidson, C. M. Sadowski, and H. I. Schiff

York University, Toronto, Ontario, Canada

G. E. Streit,* Carleton J. Howard, D. A. Jennings,† and A. L. Schmeltekopf

Aeronomy Laboratory, NOAA Environmental Research Laboratories, Boulder, Colorado 80302

(Received 25 August 1975)

Absolute rate constants for the deactivation of $O(^1D)$ atoms by some atmospheric gases have been determined by observing the time resolved emission of $O(^1D)$ at 630 nm. $O(^1D)$ atoms were produced by the dissociation of ozone via repetitive laser pulses at 266 nm. Absolute rate constants for the relaxation of $O(^1D)$ ($\times 10^{-10}$ cm³ molecule⁻¹ s⁻¹) by $N_2(0.30 \pm 0.01)$, $O_2(0.41 \pm 0.05)$, $CO_2(1.2 \pm 0.09)$, $O_3(2.4 \pm 0.1)$, $H_2(1.3 \pm 0.05)$, $D_2(1.3 \pm 0.05)$, $CH_4(1.3 \pm 0.3)$, $HCl(1.4 \pm 0.3)$, $NH_3(3.4 \pm 0.3)$, $H_2O(2.1 \pm 1.0)$, $N_2O(1.4 \pm 0.1)$, and Ne (< 0.0013) are reported at 298 K. The results obtained are compared with previous relative and absolute measurements reported in the literature.

INTRODUCTION

During the past few years there has been increasing concern over possible depletion of the earth's ozone shield as a result of human activity. In order to predict the chemical effects of such activity it is necessary to understand the chemistry of the unperturbed stratosphere. It is now reasonably well established that the ozone budget is mainly controlled by reactions with the oxides of nitrogen (NO_x) in the lower and midstratosphere and by reactions involving HO_x radicals (HO , HO_2) in the upper stratosphere and mesosphere. These reactive species derive mainly from reactions of $O(^1D_2)$ atoms, with N_2O , in the case of NO_x , and with H_2O , CH_4 , and H_2 in the case of HO_x . The $O(^1D_2)$ atoms are produced by the uv photolysis of O_3 and are lost mainly by nonreactive quenching collisions with N_2 and O_2 . Reactions of $O(^1D_2)$ atoms are, therefore, of primary importance in initiating stratospheric chemistry. Accurate reaction rate data are needed, not only on those reactions which produce reactive species but also on the competing quenching reactions.

The current status of $O(^1D_2)$ reaction rate data has been the subject of several excellent reviews.¹⁻³ The long radiative lifetime (~ 100 s) and high probability of deactivation of $O(^1D_2)$ by all convenient photolytic source gases have made the detection of the familiar red lines [$O(^1D_2) \rightarrow O(^3P_{3/2,1/2})$] very difficult in the laboratory. Therefore, most previous studies have relied on product analysis from competitive reactions to provide relative rate constants.¹ A number of absolute rate constants have been obtained by a variety of spectroscopic techniques including the time resolved $O(^3^1D_2) \rightarrow O(^2^1D_2)$ absorption at 115.2 nm,⁴⁻⁷ the intermediate quantum yield of O_3 decomposition,⁸⁻¹⁰ the decrease in $O(^1D)$ emission intensity^{11,12} and the time resolved decay of $O(^1D)$ emission.¹³ The most comprehensive study has been that of Husain and co-workers who have reported rate constants for 18 gases to date. The technique employed in the present study most closely resembles the direct technique of Gilpin *et al.*¹³ with the major difference being the use of a laser as the photolysis light source instead of a continuous light source. This provided the major advantage of a much shorter light pulse

thereby permitting much better time resolution. This paper reports measurements of absolute rate constants for the quenching of $O(^1D)$ with 12 simple gases of interest in the earth's atmosphere, including NH_3 for which no measurements have been reported, and HCl for which no absolute measurements are available.

EXPERIMENTAL

The apparatus employed in this study is shown schematically in Fig. 1. It is best described by discussing separately each of its three major components.

The laser

The photolytic source is a frequency quadrupled neodymium-YAG (Nd-YAG) laser. The Nd-YAG crystal is excited by a xenon flash lamp having an input energy adjustable from 10-29 J. Both the flash lamp and the laser crystal are cooled with rapidly circulated, deionized, water and are enclosed in a gold-coated, elliptical reflector in order to maximize the efficiency of excitation of the Nd-YAG crystal. A polarizer within the laser cavity insures that the polarization of the fundamental laser beam is in the horizontal plane. The pulse frequency can be varied from 10-50 s⁻¹ with a pulse energy in the fundamental mode of about 120 mJ and pulse length of about 10 ns.

A reproducible number of laser pulses is obtained by means of a photodiode attached to the outside of the flash lamp housing assembly and connected to a pulse counter which allows the number of pulses to be preset in integral multiples of 1024.

Two doubling crystals are used in the optical train—a CD*A crystal which doubles the 1064 nm infrared fundamental which, in turn, is doubled by an ADP crystal to yield 266 nm radiation. This quadrupled radiation has a maximum beam diameter of about 4 mm. Since each of these crystals produces output radiation with the plane of polarization rotated by 90° to the incident beam, polarizers are used after each doubling stage to remove the incident radiation which has traversed the crystal. Because the efficiencies of the doubling crystals are very sensitive to temperature, they are housed

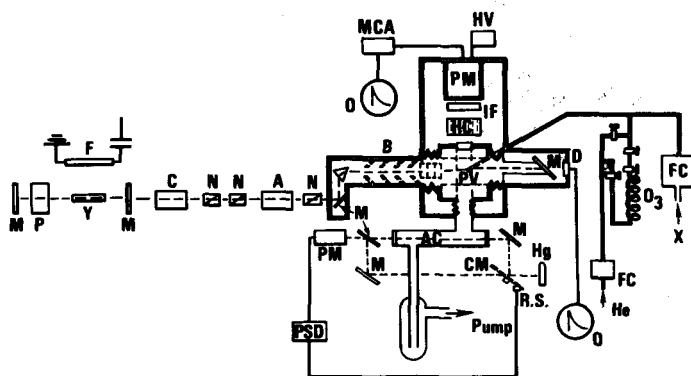


Fig. 1. Schematic diagram of apparatus used for $O(^1D)$ absolute rate constant measurements. F—flash lamp, Y—Nd:YAG rod, P—Pockels cell, M—mirror, C—CD*A crystal, A—ADP crystal, N—polarizer, B—baffles, PV—reaction volume, HC—honeycomb filter, IF—6300 Å interference filter, PM—photomultiplier tube, HV—high voltage supply, MCA—1 μ sec resolution multichannel analyzer, O—oscilloscope, Hg—mercury lamp, CM—chopper mirror, R.S.—reference signal, AC—absorption cell, PSD—phase sensitive detector, FC—flow controllers.

in well insulated temperature controlled ovens. Minor modifications of the ovens provided by the manufacturer were found to be necessary in order to achieve the thermal stability required for maximum efficiency. Since CD*A crystals degrade in an oxygen atmosphere the oven for that crystal was modified to provide a constant flow of dry nitrogen gas around the crystal. The doubling efficiency obtained was somewhat less than the 20% expected for each crystal and the energy of 266 nm radiation obtained was only about 1 mJ. Between 2048 and 10240 laser pulses were required to generate each $O(^1D)$ decay curve, the larger number being required as the flash lamp approached the end of its useful life.

Since the polarizers are not 100% efficient in removing the 1064 and 532 nm radiation, the laser beam is passed through a baffled prism monochromator before entering the photolysis cell.

The photolysis cell

When irradiated with the uv pulse the suprasil entrance and exit windows were found to exhibit a spectrally broad long-lived fluorescence. To minimize this effect an internal baffle system was incorporated into the cell and the exit window was mounted at the Brewster angle on a light exit tube in order to minimize back reflection. The relative intensity of the 266 nm radiation was monitored by a Si photodetector at the end of the exit tube.

The photolysis cell itself was constructed from a single stainless steel block by machining three orthogonal 5 cm diam holes through the block. This cell is housed in an evacuated brass chamber for thermal insulation and is connected to it by stainless steel bellows to provide for thermal expansion.

A photomultiplier (S-20 type cathode) is also housed

in the vacuum chamber to detect 630 nm ($O(^1D) \rightarrow O(^3P)$) radiation. The photomultiplier is directed at right angles to the laser beam through one of the 5 cm diam holes, and is cooled to 193 K to minimize dark current. A collimator (5° acceptance angle) and an interference filter (centered at 630 nm, 85% peak transmission, 1.5 nm half-peak width) are placed in front of the photomultiplier in order to discriminate against scattered light, window fluorescence, and O_3 induced chemiluminescence. The photomultiplier output is detected by photon counting with an amplifier discriminator and the pulses are stored in a multichannel analyzer having a minimum channel width of 1 μ sec. The output may be displayed on an oscilloscope for photographing or transferred to magnetic tape for subsequent analysis.

Gas flow system

Ozone is prepared by discharging ultrahigh purity O_2 in a commercial ozonizer. The O_2 - O_3 mixture thus produced is trapped on silica gel at 193 K and purified by pumping on the trap until the measured concentration of O_3 evolved agrees with the total system pressure within 5%. The O_3 thus purified is eluted at low pressures by a small flow of He to produce a partial pressure of O_3 in the reaction cell in the range 5–50 mTorr. The O_3 concentration is measured after exiting from the photolysis cell by monitoring the absorption of 2537 Å radiation in a dual beam absorption apparatus equipped with differential phase sensitive detection. The pressure in the cell was kept constant in the range from 1–30 Torr by bypassing the major portion of the carrier flow past the silica gel trap. Helium was the carrier gas generally used. However during the experiments in which H_2 , NH_3 , CH_4 , HCl , and N_2O quenching was being studied radiation was observed at 630 nm which was believed to be caused by emission from excited states formed in secondary reactions (*vide infra*). In these cases SF_6 was used as the carrier because of its known efficiency for vibrational relaxation, although He was still used to elute the O_3 from the silica gel trap. He and SF_6 have very low quenching efficiencies for $O(^1D)$ and serve the purposes of reducing diffusion to the walls, of preventing temperature increases due to the laser pulse or exothermic processes, and of thermalizing any translationally "hot" $O(^1D)$ atoms which may be produced by O_3 photolysis. The carrier gas, maintained at a constant pressure during the experiment, flowed through the cell at a rate sufficient to ensure replacement of the cell capacity within a few laser pulses. The carrier and quenching gases were each metered into the cell through calibrated flow elements for which the back pressures were maintained at exactly 760 Torr by servo pressure controllers. The flow metering systems were calibrated by measuring the pressure increase in a calibrated volume with a capacitance manometer.

The gases were commercial grades stated by the manufacturer to have the following purities: He, 99.999%; Ne, 99.99%; O_2 , 99.99%; N_2 , 99.999%; CO_2 , 99.99%; N_2O , 98.0%; CH_4 , 99.99%; HCl , 99.0%; D_2 , 99.5%; H_2 , 99.999%; NH_3 , 99.9%; SF_6 , 99.99%. They were all used with no further purification.

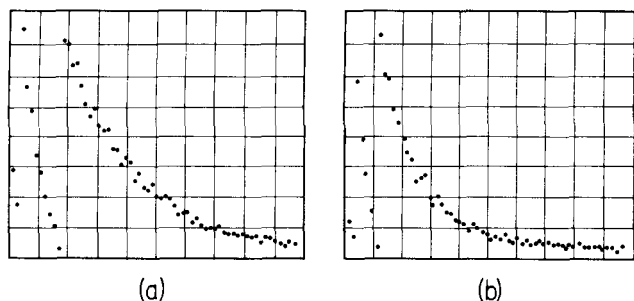


Fig. 2. Traces of O(¹D) emission decay. Time scale = 1 μ s/pt. The initial points on each plot represent 4 times and 2 times (left to right) the scale of the remaining decay curve. (a) SF₆: 12.5 Torr, O₃: 2.2×10^{14} molecules/cm³; (b) SF₆: 12.5 Torr, O₃: 2.2×10^{14} molecules/cm³, N₂O: 4.0×10^{14} molecules/cm³.

RESULTS AND DISCUSSION

Reaction of O(¹D) with O₃

These experiments were performed by irradiating the O₃ in a He carrier with a 10 nsec pulse at 266 nm. The O(¹D) atoms formed by the O₃ photolysis were observed by the emission of the O(¹D)–O(³P) emission at 630 nm/starting within 1 μ sec of the laser pulse. The decay of the emission with time provides a measure of the rate of reaction of O(¹D) with O₃. Because the probability of emission from O(¹D) is very low, it was necessary to use repetitive laser pulses and signal averaging techniques to obtain good time resolved decay curves such as that shown in Fig. 2.

The analysis of such data is quite straightforward. If the reaction of O(¹D) with O₃ is the only significant second order process removing O(¹D) the decay will be given by the rate equation

$$-\frac{dI}{dt} = -\frac{d[\text{O}(\text{}^1\text{D})]}{dt} = (k_1 + k_2 [\text{O}_3])[\text{O}(\text{}^1\text{D})] = k[\text{O}(\text{}^1\text{D})], \quad (1)$$

where I is the emission intensity, k_2 is the rate constant for the O(¹D) + O₃ reaction, and k_1 is the rate constant for all first order loss processes such as diffusion out of the reaction volume and deactivation on the wall. The experimental conditions were maintained

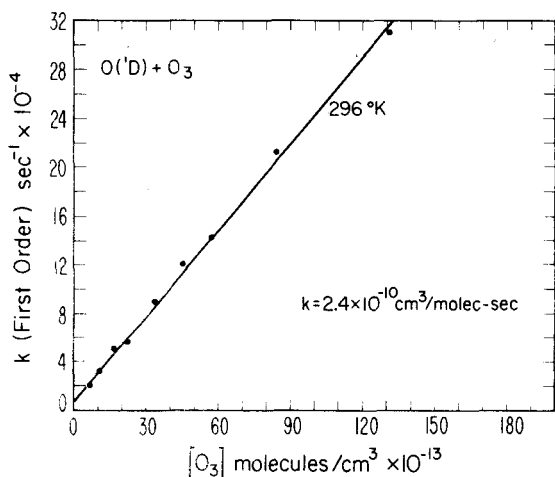


Fig. 3. Plot of first order rate constants versus ozone concentration. O₃.

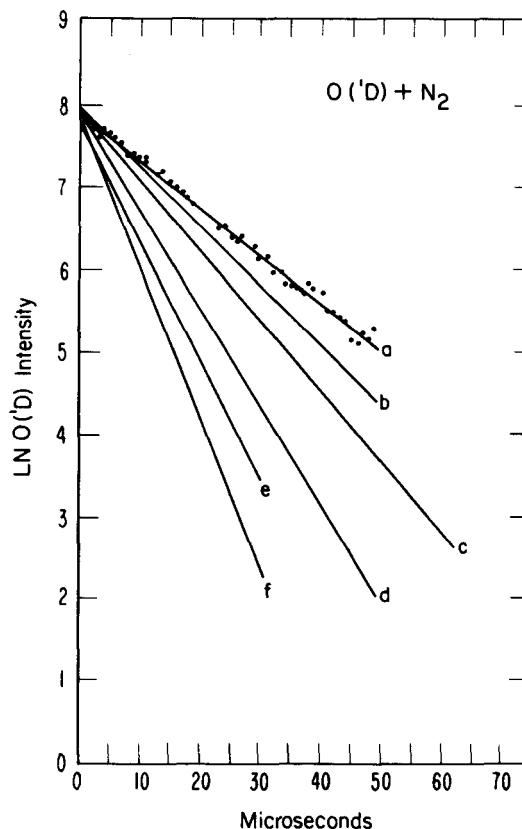


Fig. 4. Plots of $\ln \text{O}(\text{}^1\text{D})$ intensity vs. time. He = 1 Torr, O₃ = 2.33×10^{14} molecules/cm³. (a) N₂ = 0. (b) N₂ = 4.64×10^{14} molecules/cm³. (c) N₂ = 9.31×10^{14} molecules/cm³. (d) N₂ = 1.86×10^{15} molecules/cm³. (e) N₂ = 2.96×10^{15} molecules/cm³. (f) N₂ = 4.15×10^{15} molecules/cm³.

to keep [O₃] constant and much greater than [O(¹D)] , so the reaction between O(¹D) and O₃ is pseudo-first order and the overall decay rate of O(¹D) can be represented as having an "effective" first order rate constant k .

Rearrangement and integration of the rate equation from $t=0$ to $t=t$ gives

$$\ln I = \ln \frac{[\text{O}(\text{}^1\text{D})]_t}{[\text{O}(\text{}^1\text{D})]_0} = -kt + c. \quad (2)$$

Therefore a plot of $\ln I$ vs t will provide a value of the effective first order rate constant, k . From Expression (1) it will be apparent that a plot of k obtained from a number of such experiments against the O₃ concentration should yield a straight line with a slope equal to k_2 and intercept equal to k_1 . Such a plot is shown in Fig. 3.

Quenching reactions with other molecules

For quenchers other than O₃, experiments of the type outlined above are repeated in which the concentration of the quencher is varied while the concentration of O₃ is kept fixed. Under these conditions the rate expression becomes

$$-\frac{dI}{dt} = -\frac{d[\text{O}(\text{}^1\text{D})]}{dt} = (k_1 + k_2 [\text{O}_3] + k_q [\text{Q}])[\text{O}(\text{}^1\text{D})] = k'[\text{O}(\text{}^1\text{D})]. \quad (3)$$

The "effective" first order rate constant k' can be determined from a $\ln I$ vs t plot as shown in Fig. 4 in the

case of N_2 . A plot of k' vs $[Q]$ should again yield a straight line, as illustrated in Fig. 5 (a)–(c) for various quenchers, with the slope equal to k_q , but, in this case, the intercept will equal $k_1 + k_2[O_3]$.

To assess the accuracy of the work it is necessary to consider possible systematic errors. First, it is nec-

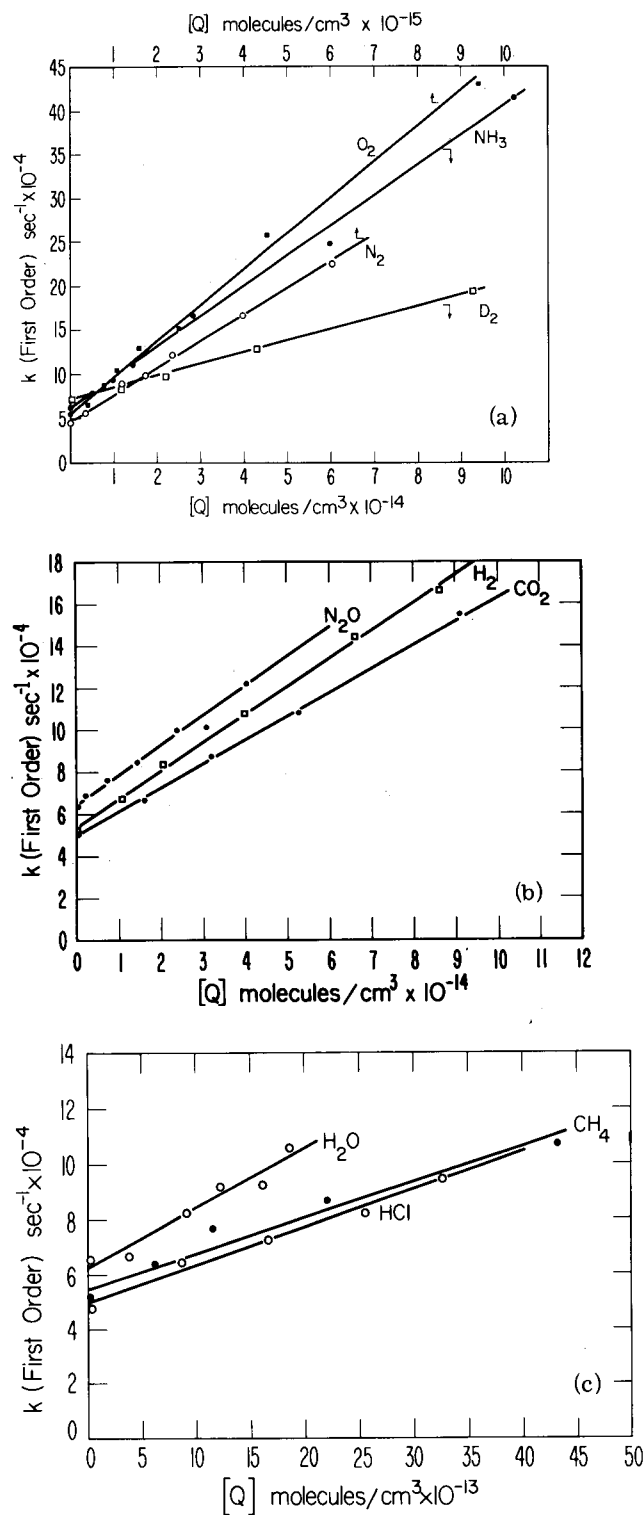


Fig. 5. Plots of first order rate constants vs quencher concentration. (a) O_2 , N_2 , NH_3 , D_2 . (b) N_2O , H_2 , CO_2 . (c) H_2O , CH_4 , HCl .

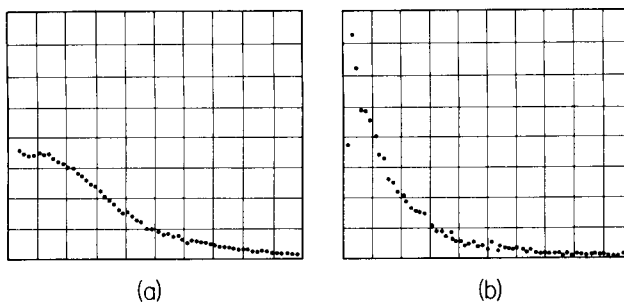


Fig. 6. Experimental decay traces exhibiting quenching of secondary emission in $O(^1D) + NH_3$. Time scale = $1 \mu\text{s}/\text{pt}$. (a) He: 1 Torr, O_3 : 2.4×10^{14} molecules/ cm^3 , NH_3 : 1.8×10^{13} molecules/ cm^3 , (b) SF_6 : 22.5 Torr, O_3 : 2.2×10^{14} molecules/ cm^3 , NH_3 : 1.4×10^{14} molecules/ cm^3 .

essary to ensure that the emission observed is due solely to $O(^1D)$. In the absence of quencher other than O_3 a large decrease in intensity was observed when the interference filter was tilted a few degrees, as would be expected for a sharp atomic emission and a narrow bandpass filter. This was also found to be the case when the quenching gases N_2 , O_2 , D_2 , and CO_2 were present. However, other emissions were observed when some of the other gases were present. These emissions appear at different times after the laser pulse. In the case of NH_3 and H_2 , the intensity increases after the pulse and then decreases so that the overall curve is no longer exponential. An example of such behavior for NH_3 is shown in Fig. 6(a). The magnitude of this secondary emission is much smaller for CH_4 and HCl . We suspect that this secondary emission is due to vibrationally excited secondary species. Support for this conjecture is provided by the disappearance of this emission when SF_6 is added, as shown in Fig. 6(b). SF_6 is known to be effective in relaxing vibrational excitation. The secondary emission observed with H_2 is believed to be the (9-3) OH Meinel band in the 630 nm region. This is supported by the fact that no secondary emission was observed with D_2 because there are no strong vibrational bands of OD in the spectral region viewed by the detector. In the case of N_2O the secondary emission occurred rapidly after the laser pulse so that an apparent exponential decay was obtained under most conditions. The decay rate however increased when SF_6 was used as the carrier gas and was independent of SF_6 pressure above 5 Torr as shown in Table I. Apparently the secondary emission in this case also involved vibrationally excited species which were effectively relaxed by SF_6 .

TABLE I. Pressure dependence of $O(^1D) + N_2O$ rate constant.

Buffer gas	Buffer pressure (Torr)	Noticeable secondary emission	k ($\text{cm}^3 \text{ molecule}^{-1} \cdot \text{s}^{-1}$)
He	1	Yes	6.7×10^{-11}
SF_6	0.27	Yes	4.4×10^{-11}
SF_6	0.83	Yes	1.1×10^{-10}
SF_6	5	No	1.5×10^{-10}
SF_6	10.2	No	1.6×10^{-10}
SF_6	12.5	No	1.4×10^{-10}
SF_6	33.8	No	1.4×10^{-10}

may be found in most statistics texts.¹⁸ Except for the cases of CH_4 , HCl , and H_2O , the precision is quite good and considering the earlier discussion of systematic errors we feel confident that the accuracy of our data is within $\pm 15\%$. For CH_4 and HCl problems arose with secondary emission and for H_2O with obtaining a sufficient range of reactant concentration so for these cases we judge our accuracy to be only $\pm 40\%$ – 50% . Further experiments will be conducted with these three gases.

Also shown in Table III are the absolute rate constants obtained by other workers. Row 1 gives the absolute values recommended by Cvetanovic,¹ CIAP,³ and NBS,² which were obtained in the following manner. The relative values were combined with the absolute values reported in the literature to compute a set of mean values, which formed the basis of the "recommended" values appearing in row 1 along with "a somewhat arbitrary but hopefully conservative estimate of their likely total uncertainties". Since virtually all the absolute values used as the basis for these "recommended values" are those of Husain and co-workers⁴⁻⁷ they are obviously heavily weighted by the results of this group. The agreement between various workers on the rate constants for O_3 is excellent, although the accuracy of these measurements might be expected to be the lowest both because the determination of the absolute concentration of O_3 is less accurate than those of the more stable quenchers and because in this case O_3 is used both as the source of $O(^1D)$ and as the quencher. Unfortunately the agreement for the other quenchers is not nearly as good between our values and those of Husain and coworkers who have made the bulk of the previous absolute rate constant measurements. The method used by this group involves detection of $O(^1D)$ by resonance absorption which necessitated the introduction of a factor γ equal to 0.41 to correct for deviation from Beer's law due to optical thickness. It is interesting to note that had a value of $\gamma = 0.7$ been used in their calculations the values in row 7 would have been obtained which would be in agreement with our results within the combined uncertainties for all the quenchers with the exception of O_3 .

Note added in proof. We wish to thank Professor L. F. Phillips for informing us prior to publication of the

results of his calculation of γ for $O(^1D)$ absorption. His calculations [Chem. Phys. Lett. (in press)] predict that a larger γ factor than that used by Husain and co-workers is appropriate, resulting in a reduction factor for their rate constants of 2.2 ± 0.4 . The reduced rate constants would be in very good agreement with the results reported here.

ACKNOWLEDGMENT

We acknowledge that part of this work was supported by NASA through NASA contract #NGR 52-134-005.

* NRC NOAA Postdoctoral Fellow.

† National Bureau of Standards, Boulder, Co.

¹R. J. Cvetanovic, Can. J. Chem. 53, 1452 (1974).

²D. Garvin and R. F. Hampson, Editors, NBSIR 74-430 (1974).

³Department of Transportation, Climatic Impact Assessment Program, Monograph No. 1 (1974).

⁴R. F. Heidner III, D. Husain, and J. R. Wiesenfeld, Chem. Phys. Lett. 16, 530 (1972).

⁵R. F. Heidner III and D. Husain, Nature Phys. Sci. 241, 10 (1973).

⁶R. F. Heidner III and D. Husain, Int. J. Chem. Kinet. 5, 819 (1973).

⁷R. F. Heidner III and D. Husain, Int. J. Chem. Kinet. 6, 77 (1974).

⁸D. Biendenkapp, L. G. Hartshorn, and E. J. Bair, Chem. Phys. Lett. 5, 379 (1970).

⁹D. R. Snelling and E. J. Bair, J. Chem. Phys. 47, 228 (1967).

¹⁰D. R. Snelling and E. J. Bair, J. Chem. Phys. 48, 5737 (1968).

¹¹J. F. Noxon, J. Chem. Phys. 52, 1852 (1970).

¹²I. D. Clark and J. F. Noxon, J. Chem. Phys. 57, 1033 (1973).

¹³R. Gilpin, H. I. Schiff, and K. H. Welge, J. Chem. Phys. 55, 1087 (1971).

¹⁴G. A. Chamberlain and J. P. Simons, J. C. S. Faraday II, 71, 402 (1975).

¹⁵M. J. Kurylo, W. Braun, A. Kaldor, S. M. Freund, and R. P. Wayne, J. Photochem. 3, 71 (1975).

¹⁶R. J. Gordon and M. C. Lin, Chem. Phys. Lett. 22, 262 (1973).

¹⁷M. J. E. Gauthier and D. R. Snelling, J. Photochem. 4, 27 (1975).

¹⁸N. R. Draper and H. Smith, *Applied Regression Analysis* (Wiley, New York (1966)).